

# Construction of a D-Amino Acid Oxidase Reactor Based on Magnetic Nanoparticles Modified by a Reactive Polymer and Its Application in Screening Enzyme Inhibitors

Xiaoyu Mu,<sup>†,‡</sup> Juan Qiao,<sup>†</sup> Li Qi,<sup>\*,†</sup> Ying Liu,<sup>§</sup> and Huimin Ma<sup>†</sup>

<sup>†</sup>Beijing National Laboratory for Molecular Sciences, Key Laboratory of Analytical Chemistry for Living Biosystems, Institute of Chemistry, Chinese Academy of Sciences, Beijing 100190, P.R. China

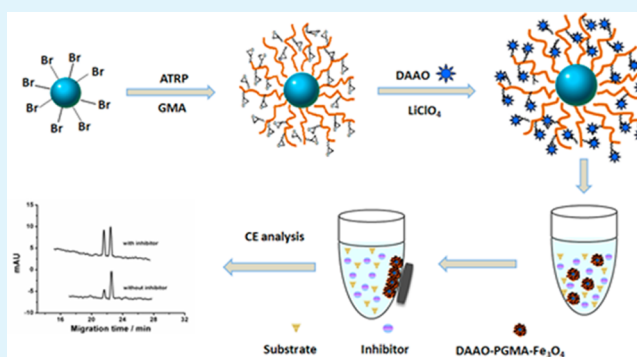
<sup>‡</sup>Graduate School, University of Chinese Academy of Sciences, Beijing 100049, P.R. China

<sup>§</sup>College of Life and Environment Science, Minzu University of China, Beijing 100018, P.R. China

## Supporting Information

**ABSTRACT:** Developing facile and high-throughput methods for exploring pharmacological inhibitors of D-amino acid oxidase (DAAO) has triggered increasing interest. In this work, DAAO was immobilized on the magnetic nanoparticles, which were modified by a biocompatible reactive polymer, poly(glycidyl methacrylate) (PGMA) via an atom transfer radical polymerization technique. Interestingly, the enzyme immobilization process was greatly promoted with the assistance of a lithium perchlorate catalyst. Meanwhile, a new amino acid ionic liquid (AAIL) was successfully synthesized and employed as the efficient chiral ligand in a chiral ligand exchange capillary electrophoresis (CLE-CE) system for chiral separation of amino acids (AAs) and quantitation of methionine, which was selected as the substrate of DAAO. Then, the apparent Michaelis–Menten constants in the enzyme system were determined with the proposed CLE-CE method. The prepared DAAO-PGMA-Fe<sub>3</sub>O<sub>4</sub> nanoparticles exhibited excellent reusability and good stability. Moreover, the enzyme reactor was successfully applied in screening DAAO inhibitors. These results demonstrated that the enzyme could be efficiently immobilized on the polymer-grafted magnetic nanoparticles and that the obtained enzyme reactor has great potential in screening enzyme inhibitors, further offering new insight into monitoring the relevant diseases.

**KEYWORDS:** enzyme immobilization, D-amino acid oxidase, magnetic nanoparticles, polymer, screening inhibitors



## 1. INTRODUCTION

D-Amino acid oxidase (DAAO) is a well characterized FAD-dependent flavoenzyme which catalyzes the stereospecific oxidative deamination of D-amino acids (D-AAAs) to the corresponding  $\alpha$ -keto acids, hydrogen peroxide, and ammonia.<sup>1,2</sup> D-AAAs play an increasingly important role in the regulation of many processes in living cells, including aging, neural signaling, and hormone secretion.<sup>3</sup> For example, D-serine, which is a significant endogenous neurotransmitter in the central nervous system, was reported to improve negative symptoms and cognitive impairments of schizophrenia. The decreased cerebrospinal fluid concentration of D-serine has been considered to underlie some of the behavioral and neurobiological deficits related to schizophrenia.<sup>4–6</sup> Since the main metabolic oxidation of D-serine in mammals is mediated by DAAO, the inhibition of DAAO has attracted substantial interest as an available way to increase D-serine levels in the brain. During the past decades, a great number of structurally diverse DAAO inhibitors have been identified with favorable inhibitory potency.<sup>7–12</sup> Subsequently, several protocols, includ-

ing a colorimetric method and a fluorometric assay were explored for the screening and discovery of DAAO inhibitors.<sup>8–12</sup> However, these methods have some inherent drawbacks in that (1) a suitable colorimetric or fluorometric reagent must be available to generate a signal; (2) interferences can arise from tangled multireactions and various compounds; (3) these methods are mainly carried out with free enzyme solutions and thus are often hampered by the low operational stability and difficulties in recovery and reuse; and that (4) complex and special manipulation was required through the pretreatment process.<sup>12–14</sup> Therefore, exploration of a simple and efficient approach to improve the stability and reusability of DAAO for screening enzyme inhibitors is essential and pressing.

The immobilization of enzymes usually exhibits several advantages over free enzymes, such as much higher stability,

Received: May 12, 2014

Accepted: July 1, 2014

Published: July 1, 2014

increased convenience in handling, easier separation from the product, and increased efficiency in recovery and reuse of those costly enzymes.<sup>15,16</sup> Since the source of DAAO is quite limited and its native activity in solutions is likely to be decreased, enzyme immobilization is a fascinating alternative. López-Gallego and colleagues have successfully immobilized DAAO on sephabeads with covalent attachment using glutaraldehyde as the cross-linker with a maximum load capacity of 15.0  $\mu\text{g}/\text{mg}$  sephabeads.<sup>17</sup> Bava and co-workers have functionalized  $\text{Fe}_3\text{O}_4$  nanoparticles with 3-aminopropyltriethoxysilane (APTES) and conjugated it to DAAO by coupling this with glutaraldehyde. The amount of enzyme bound to nanoparticles is approximately 70% (43.8  $\mu\text{g}/\text{mg}$  nanoparticles).<sup>18</sup> Marinesco and colleagues have fabricated the microelectrode biosensor based on covalent immobilization of DAAO using poly(ethylene glycol) diglycidyl ether (PEGDE).<sup>19</sup> However, these reported immobilization techniques of DAAO exhibited some limitations as presented in the following: (1) the species of available cross-linkers were limited within glutaraldehyde or PEGDE; (2) there were restricted interaction sites for enzyme immobilization, resulting in low loading capacity;<sup>20</sup> and (3) the reaction process was complicated, and long immobilization time was required. Thus, it is of great significance to explore new materials for effectively immobilizing the DAAO enzyme in high capacity.

With the rapid development of nanotechnology, immobilization of enzymes has been performed on various nanomaterials, such as nanoparticles, mesoporous materials, nanofibers, and single enzyme nanoparticles.<sup>21</sup> Among all of these nanomaterials, one of the most available strategies is the construction of reactive polymer modified magnetic nanoparticles, which can possess a large amount of active sites on the polymer shells and combine the advantages of easy separation from the reaction medium and high loading capacity.<sup>22</sup> It has been reported that a variety of polymer brushes, such as poly(acrylic acid), poly[(glycidyl methacrylate)-*co*-(glycerol monomethacrylate)], and poly(glycidyl methacrylate) (PGMA), have been successfully modified onto the surface of the magnetic particles for enzyme immobilization.<sup>22–27</sup> However, the applications of these as-prepared polymer-functionalized magnetic particles are mostly limited in protein digestion. Moreover, so far to our knowledge, only few of the polymer-modified magnetic nanoparticles have been explored for efficiently screening enzyme inhibitors. Considering that the flexible non-cross-linked polymer chains of PGMA could not only afford a tremendous amount of reactive sites but also act as the effective scaffold to support three-dimensional enzyme immobilization, resulting in increasing the loading capacity and improving the accessibility of the immobilized enzyme, PGMA-grafted magnetic nanoparticles are speculated to have great potential for application in screening enzyme inhibitors.

In this work, PGMA brushes were modified onto the magnetic nanoparticles via the atom transfer radical polymerization (ATRP) technique, and then DAAO was immobilized on the resulting magnetic nanoparticles (PGMA- $\text{Fe}_3\text{O}_4$ ), further applied in screening DAAO inhibitors. Considering that the long immobilization time might lead to loss in DAAO enzyme activity, lithium perchlorate ( $\text{LiClO}_4$ ) was thus employed as the catalyst to promote the immobilization process since it could effectively catalyze the ring opening of epoxides with amines to provide the corresponding  $\beta$ -aminoalcohols in excellent yields.<sup>28–30</sup> Meanwhile, a new chiral ligand-exchange capillary electrophoresis (CLE-CE) system with amino acid ionic liquid (AAIL) as the chiral ligand was

developed to study the enzymolysis of immobilized DAAO on the basis of monitoring the concentration change of the substrate methionine (Met), due to its advantages of high convenience, high efficiency, high speed, and low cost.<sup>31,32</sup> Furthermore, the prepared magnetic DAAO-PGMA- $\text{Fe}_3\text{O}_4$  nanoparticles as the enzyme reactor were applied in studying the inhibition efficiency of classical DAAO inhibitors including benzoic acid and various monosubstituted benzoic acid derivatives.

## 2. EXPERIMENTAL SECTION

**2.1. Chemicals.** L-Ornithine (L-Orn) and other amino acid (AA) enantiomers, bromophenol blue,  $\beta$ -mercaptoethanol, glycerol, sodium dodecyl sulfate (SDS), dansyl chloride (Dns-Cl), and DAAO (from porcine kidney) were purchased from Sigma-Aldrich Chemical Co. (St. Louis, USA). Dimethyl-*d*<sub>6</sub> sulfoxide was obtained from Cambridge Isotope Laboratories (Massachusetts, USA). *N*-Butyl-*N*-methyl-piperidinium bromide ( $[\text{P}_{1,4}][\text{Br}]$ ) was supplied by Lanzhou Institute of Chemical Physics (Lanzhou Greenchem ILS, LICP, CAS, P.R. China). Glycidyl methacrylate (GMA) was obtained from Acros (New Jersey, USA). Ferric chloride hexahydrate ( $\text{FeCl}_3 \cdot 6\text{H}_2\text{O}$ ) was purchased from Xilong Chemical Company (Guangdong, P.R. China). Ferrous chloride tetrahydrate ( $\text{FeCl}_2 \cdot 4\text{H}_2\text{O}$ ) was purchased from Tianjin Damao Chemical Reagent Factory (Tianjin, P.R. China). Coomassie brilliant blue G-250, lithium perchlorate ( $\text{LiClO}_4$ ),  $\alpha$ -bromoisobutyric acid (BIB), benzamide, benzoic acid, 4-hydroxybenzoic acid, 3-hydroxybenzoic acid, 2-hydroxybenzoic acid, 4-aminobenzoic acid, 2-aminobenzoic acid, 4-nitrobenzoic acid, 3-nitrobenzoic acid, and 2-nitrobenzoic acid were purchased from Aladdin Chemistry Company (Shanghai, P.R. China). Zinc sulfate, tris (hydroxymethyl) amino-methane (Tris), cuprous bromide (CuBr), lithium carbonate, sodium chloride, sodium hydroxide, boric acid, hydrochloric acid, anhydrous ethanol, methanol, tetrahydrofuran (THF), cyclohexanone, 2,2'-bipyridyl (bpy), and other reagents were all purchased from Beijing Chemical Factory (Beijing, P.R. China). The PageRuler prestained protein ladder was purchased from Thermo Fisher Scientific Company (Massachusetts, USA). CuBr was rinsed by acetic acid and methanol in turn before use. All of the chemical reagents used in this work were of analytical grade.

**2.2. Instrumentation.** Gel permeation chromatography (GPC) measurements were conducted on a Waters 1515 HPLC solvent pump, which was equipped with a Waters 2414 differential refractometer detector and a set of Waters Styragel columns with THF as the eluent at a flow rate of 1.0 mL/min. The Fourier transform infrared (FT-IR) spectra were recorded on a Bruker Tensor-27 spectrophotometer at wavenumbers ranging from 4,000 to 400  $\text{cm}^{-1}$  under ambient conditions. Transmission electron microscope (TEM) images were taken on a JEOL JEM-2010 high-resolution TEM at an acceleration voltage of 200 kV. Magnetic characterization was performed on a Lakeshore 7307 vibrating sample magnetometer (VSM). All of the separation experiments were performed on a capillary electrophoresis (CE) system consisting of a UV detector (Rilips Photoelectricity Factory, Beijing, China), a 1229 HPCE high voltage power supply (Beijing Institute of New Technology and Application, Beijing, China), a HW-2000 chromatography workstation (Qianpu software, Nanjing, China), and uncoated bare capillaries of 60 cm (effective length 45 cm)  $\times$  75  $\mu\text{m}$  i.d. (Yongnian Optical Fiber Factory, Hebei, China).

**2.3. Preparation of DAAO-PGMA- $\text{Fe}_3\text{O}_4$  Nanoparticles.**  
**2.3.1. Preparation of Br- $\text{Fe}_3\text{O}_4$  Nanoparticles.** Alkaline precipitation of magnetic  $\text{Fe}_3\text{O}_4$  nanoparticles was conducted according to the method described by Massart and Cabuil.<sup>33</sup> The aqueous suspension was rinsed repeatedly with distilled water and methanol. Then per gram of fresh particles was reacted with 1.67 mmol (277.2 mg) of BIB for 24 h under vigorous agitation and then washed with methanol several times, followed by evaporation at 50  $^\circ\text{C}$  under vacuum to obtain BIB-functionalized  $\text{Fe}_3\text{O}_4$  nanoparticles (Br- $\text{Fe}_3\text{O}_4$  nanoparticles).

**2.3.2. Preparation of PGMA-Fe<sub>3</sub>O<sub>4</sub> Nanoparticles.** The PGMA-Fe<sub>3</sub>O<sub>4</sub> nanoparticles were prepared by the ATRP technique as follows: the Br-Fe<sub>3</sub>O<sub>4</sub> nanoparticles (0.3 g) as the initiator, GMA (25.0, 50.0, and 100.0 mmol, respectively) as the monomer, and CuBr/bpy (0.5 mmol/1.5 mmol) as the catalyst were dissolved in cyclohexanone (20 mL) and reacted at 55 °C for 24 h. Then, the resultant magnetic PGMA-Fe<sub>3</sub>O<sub>4</sub> nanoparticles were washed repeatedly with THF and water. It should be noted that the polymer was retrieved by acid hydrolysis for GPC characterization.

**2.3.3. Preparation of DAAO-PGMA-Fe<sub>3</sub>O<sub>4</sub> Nanoparticles.** PGMA-Fe<sub>3</sub>O<sub>4</sub> nanoparticles (10.0 mg) and 2.0 mg of LiClO<sub>4</sub> were added into 1.0 mL of DAAO solution (2.5 mg/mL, in 100.0 mM phosphate buffer, pH 8.2), and the mixture was shaken at 25 °C for 3 h. Then, the resultant magnetic DAAO-PGMA-Fe<sub>3</sub>O<sub>4</sub> nanoparticles were washed with distilled water repeatedly to remove free enzyme and stored at 4 °C in 50.0 mM Tris-HCl buffer (pH 8.2) for future use.

**2.4. Measurement of the Amount of DAAO Immobilized on Magnetic Nanoparticles.** A classical Coomassie blue binding assay was applied to determine the amount of immobilized DAAO. The dye-reagent was prepared as previously described.<sup>34,35</sup> Coomassie brilliant blue G-250 (10.0 mg) was dissolved in 5 mL of 95% ethanol. Phosphoric acid [10 mL, 85% (w/v)] was added, and the resulting solution was diluted with water to a final volume of 100 mL and filtered. After the DAAO immobilization procedure was performed, the magnetic nanoparticles were retained by a magnet. Then, the supernatant solution (20 μL) was added to the Coomassie brilliant blue G-250 solution (180 μL) and incubated for 2 min at 25 °C under shaking. The absorbance value was measured at 595 nm to calculate the amount of DAAO immobilized on the magnetic nanoparticles using a SpectraMax M5 ELISA Reader (Molecular Devices, CA, USA). For accurate calculation of the immobilized amount, a calibration curve was obtained at 595 nm by the incubation of a series of standard DAAO solutions containing different concentrations (buffered at pH 8.2) with Coomassie brilliant blue G-250 solution.

**2.5. SDS-PAGE Analysis.** In order to test whether DAAO was immobilized to the PGMA-Fe<sub>3</sub>O<sub>4</sub> nanoparticles by chemical covalent reaction or by physical absorption, 2.0 mg of DAAO-PGMA-Fe<sub>3</sub>O<sub>4</sub> nanoparticles was incubated with 100 μL of 1.0 M NaCl solution overnight to desorb the enzyme, which was immobilized by physical absorption.<sup>36</sup> Then, the supernatant was analyzed by sodium dodecyl sulfate–polyacrylamide gel electrophoresis (SDS–PAGE) according to the same step to the free enzyme as described below.

To further validate if the immobilization process of DAAO involved the full immobilization of the quaternary structure since DAAO is a multimeric enzyme, both the free DAAO and the DAAO-PGMA-Fe<sub>3</sub>O<sub>4</sub> nanoparticles were added into the buffer solution containing 50.0 mM Tris-HCl (pH 6.8), bromophenol blue (0.01%, w/v), glycerol (10%, v/v), 0.7 M β-mercaptoethanol, and SDS (1%, w/v), and then heated for 15 min at 95 °C to desorb the protein subunit, which was not immobilized to the support by a covalent bond.<sup>36,37</sup> These samples were all separated on a 10% SDS–PAGE gel with a running buffer consisted of SDS (0.1%, w/v), Tris (0.3%, w/v), and glycine (1.2%, w/v).<sup>36,37</sup> Protein bands were stained with Coomassie brilliant blue R-250.

**2.6. Measurement of DAAO Activity.** The catalytic activity of the immobilized DAAO was measured using the proposed CLE-CE method. As a typical substrate of DAAO, Met was dissolved in 50.0 mM Tris-HCl (pH 8.2) and diluted to different concentrations ranging from 0.125 mM to 2.5 mM. The enzymatic reaction was conducted in 0.5 mL polypropylene tubes containing 0.4 mg of DAAO immobilized magnetic nanoparticles and 40 μL of Met solution with various concentrations. After incubation at 37 °C for 5 min, the DAAO immobilized magnetic nanoparticles were retained by a magnet, and the supernatant solution was derived for CE analysis. The detailed derivatization procedure was shown in Supporting Information.

**2.7. Screening DAAO Inhibitors.** To screen the enzyme inhibitors, 10 kinds of classical inhibitors including benzoic acid and various monosubstituted benzoic acid derivatives were chosen. DAAO immobilized magnetic nanoparticles (0.4 mg), 40 μL of substrate solution, and 40 μL of inhibitor solutions were mixed in 0.5 mL

polypropylene tubes and incubated at 37 °C for 5 min. Each assay for all inhibitors was performed in triplicate (*n* = 3). Then, the DAAO immobilized magnetic nanoparticles were retained by a magnet, and the supernatant solutions were derived by Dns-Cl in the same manner as that for the standard AAs in Supporting Information (section 4) for CE analysis.

IC<sub>50</sub> (the concentration of inhibitor producing 50% inhibition efficiency) was measured at a constant substrate concentration of 333.3 μM with inhibitors, which ranged from 0.05 to 2 × 10<sup>4</sup> μM. Each concentration of these inhibitors was analyzed in triplicate. The dose–response curve was plotted by fitting the inhibition efficiency as a function of the concentration of inhibitor. Here, the inhibition efficiency (*I*) was estimated by the following formula according to the literature:<sup>38,39</sup>

$$I = (C_2 - C_1)/(C_0 - C_1) \quad (1)$$

in which *C*<sub>0</sub> refers to the concentration of D-Met in the absence of DAAO and the inhibitor, and *C*<sub>1</sub> and *C*<sub>2</sub> are the residual concentrations of D-Met in the absence and presence of the inhibitor, respectively.

The inhibition constant (*K*<sub>1</sub>) was determined by extrapolation of IC<sub>50</sub> values to the point of the substrate concentration of zero. Four different concentrations of substrate were incubated with these DAAO inhibitors (0.05 to 2 × 10<sup>4</sup> μM) and the immobilized enzyme, and the IC<sub>50</sub> was calculated as described above. Then *K*<sub>1</sub> was obtained on the basis of the rearranged equation reported by Cheng and Prusoff:<sup>40,41</sup>

$$IC_{50} = (K_1/K_m)[S] + K_1 \quad (2)$$

The reusability of the immobilized biocatalyst was evaluated by the relative activity (*RA*) of the enzyme reactor with D-Met as substrate as follows:

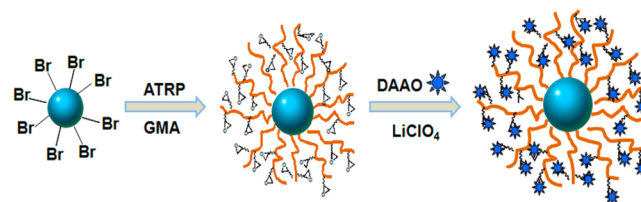
$$RA = (A_0 - A_n)/(A_0 - A_1) \quad (3)$$

where *A*<sub>0</sub> was the peak area of the substrate D-Met before enzyme digestion, *A*<sub>1</sub> and *A*<sub>*n*</sub> were the peak areas of D-Met after enzyme digestion for the first time and the *n*th time, separately.

### 3. RESULTS AND DISCUSSION

**3.1. Synthesis and Characterization of the Magnetic DAAO-PGMA-Fe<sub>3</sub>O<sub>4</sub> Nanoparticles.** The magnetic nanoparticles were synthesized with an alkaline precipitation protocol and modified by α-bromoisobutyric acid (BIB) to link ATRP initiators to the surface, which initiated the ATRP of PGMA on the surface of the magnetic nanoparticles.<sup>27,42</sup> The overall procedure is presented in Scheme 1. These as-prepared

**Scheme 1. Schematic Illustration of DAAO Immobilization onto the Reactive Polymer Modified Magnetic Nanoparticles**



PGMA-Fe<sub>3</sub>O<sub>4</sub> nanoparticles, which were grafted with different amounts of the GMA monomer, were acidolyzed for GPC measurement to evaluate the molecular weights and polymer distribution index (PDI) of PGMA homopolymers grafted onto the magnetic nanoparticle surface, and the GPC results are displayed in Table 1. The results revealed that the molecular weights increased with increasing amounts of the GMA monomer (25.0, 50.0, and 100.0 mmol), resulting in higher

**Table 1.** GPC Results of Retrieved PGMA Homopolymers and the Immobilized Amount of DAAO onto the Corresponding Magnetic Nanoparticles

sample	determined Mn	PDI	polymerization degree	total amounts of immobilized enzyme $\mu\text{g}/\text{mg}$ nanoparticle
PGMA <sub>137</sub> -Fe <sub>3</sub> O <sub>4</sub>	19534	1.73	137	94.0
PGMA <sub>157</sub> -Fe <sub>3</sub> O <sub>4</sub>	22334	1.45	157	116.0
PGMA <sub>193</sub> -Fe <sub>3</sub> O <sub>4</sub>	27487	1.78	193	222.0

polymerization degree and more reaction sites. Moreover, the prepared homopolymers exhibited low polydispersities.

It has been reported that the traditional procedure for immobilizing an enzyme onto the surface of magnetic PGMA-Fe<sub>3</sub>O<sub>4</sub> nanoparticles required quite a long time (24 h) at room temperature,<sup>27</sup> which might cause the loss of activity of some impressible enzymes. After DAAO was reacted with the PGMA-functionalized magnetic nanoparticles for 24 h, it was found that the resultant enzyme reactor showed quite low activity (7.8%). Thus, we considered improving the immobilization process. In this work, LiClO<sub>4</sub> was thus employed as the efficient catalyst for the activation of epoxides, rendering them more susceptible to nucleophilic attack under mild conditions.<sup>29,30</sup> To validate the effects of the catalyst lithium perchlorate on the specific activity of an enzyme, the control experiments were performed by comparing the activity of the free DAAO enzyme (2.5 mg/mL, in 100 mM phosphate buffer, pH 8.2) in the absence or presence of lithium perchlorate (2.0 mg). The results demonstrated that the presence of lithium perchlorate did not interfere with the enzyme and that it was in accordance with the literature.<sup>43,44</sup> The reaction time of the enzyme immobilization was investigated in detail, and the results are displayed in Figure 1. We observed that the

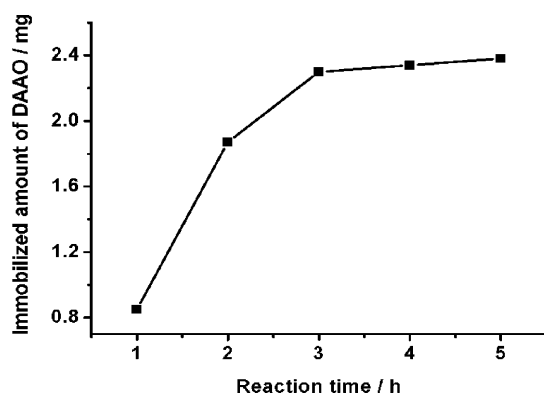


**Figure 1.** Optimization of the reaction time in the DAAO immobilization process. Conditions: 10.0 mg of PGMA-Fe<sub>3</sub>O<sub>4</sub> nanoparticles, 2.0 mg of LiClO<sub>4</sub>, and 1.0 mL of DAAO solution (2.5 mg/mL, in 100.0 mM phosphate buffer, pH 8.2) were mixed and shaken at 25 °C for different reaction times in the range of 1–5 h. The immobilized amount of DAAO was calculated according to the method described in section 2.4.

immobilized amount of enzyme remained almost constant after 3 h. Therefore, 3 h was finally adopted as the optimal reaction time. Meanwhile, the as-obtained DAAO reactor exhibited quite good activity (94.6%) for further analysis.

Moreover, to explore whether this DAAO immobilization method was really chemical covalent conjunction or just physical adsorption, here the prepared DAAO-PGMA-Fe<sub>3</sub>O<sub>4</sub>

nanoparticles were incubated with 1.0 M NaCl overnight to investigate the physical adsorption of the DAAO,<sup>36</sup> and the supernatant was analyzed by SDS–PAGE. As shown in Figure S1 (Supporting Information), none of the clear protein bands was observed after staining (lane 4). In addition, after the immobilization reaction was carried out the resultant magnetic DAAO-PGMA-Fe<sub>3</sub>O<sub>4</sub> nanoparticles were washed with the phosphate buffer solution (100.0 mM, pH 8.2) and distilled water repeatedly to remove free enzyme and avoid physical adsorption. Therefore, all these results indicated that the enzyme was covalently immobilized to the magnetic nanoparticles and that the amount of the enzyme immobilized by physical adsorption could be negligible to some extent.

Since DAAO is a multimeric enzyme, a SDS–PAGE analysis of the immobilized DAAO was performed to confirm whether the immobilization involved the full immobilization of the quaternary structure. As displayed in Figure S1 (Supporting Information), after Coomassie brilliant blue staining, there was an obvious protein band (39.3 kDa) for the prepared DAAO-PGMA-Fe<sub>3</sub>O<sub>4</sub> nanoparticles (lane 3), indicating that there were some enzyme subunits released from the magnetic nanoparticles.<sup>45,46</sup> Therefore, it was speculated that the immobilization of the DAAO enzyme might not be the full immobilization of the quaternary structure. It should be noted that faint additional bands in lanes 2 and 3 could be ascribed to the degradation products of DAAO according to the literature.<sup>47,48</sup>

FT-IR spectra were employed to confirm that PGMA has been linked on the surface of the magnetic nanoparticles. As presented in Figure 2, the characteristic absorption at 589 cm<sup>-1</sup>

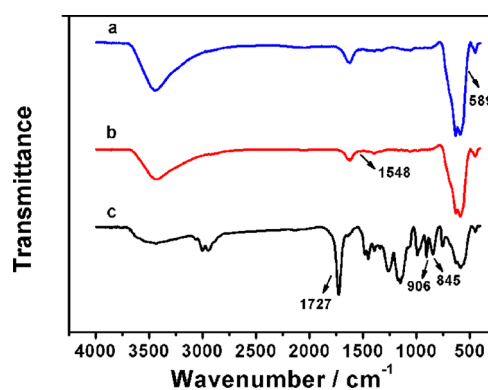


**Figure 2.** FT-IR spectra of (a) Fe<sub>3</sub>O<sub>4</sub>, (b) Br-Fe<sub>3</sub>O<sub>4</sub>, and (c) PGMA-Fe<sub>3</sub>O<sub>4</sub>.

is ascribed to the Fe–O vibrations. Compared with the free BIB ( $\nu = 1702 \text{ cm}^{-1}$ ), the vibrational absorption of the carbonyl double bond ( $\nu = 1548 \text{ cm}^{-1}$ ) of Fe<sub>3</sub>O<sub>4</sub>-Br represents a shift and an obvious decrease in intensity, while the deformational stretching absorption of the (CO)-O-H group ( $\nu = 1292 \text{ cm}^{-1}$ ) disappears, attributed to the chemisorption via the carboxylate group.<sup>42,49</sup> The peak at 1727 cm<sup>-1</sup> is the characteristic absorption of C=O stretching vibrations, and the absorption peaks at both 845 and 906 cm<sup>-1</sup> represent the existence of epoxy groups.<sup>50</sup> These FT-IR results indicated that the magnetic PGMA-Fe<sub>3</sub>O<sub>4</sub> nanoparticles were successfully synthesized.

TEM characterization was performed to investigate the morphology of the magnetic nanoparticles, and the results are shown in Figure 3. It could be found that the as-prepared Fe<sub>3</sub>O<sub>4</sub> nanoparticles were almost spherical with average diameters of

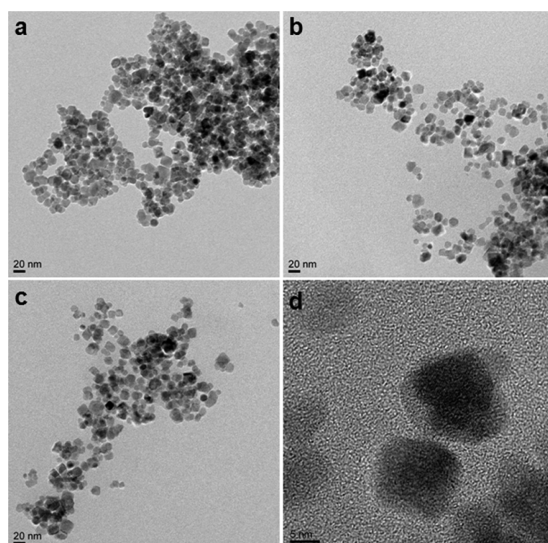


**Figure 3.** TEM images of (a)  $\text{Fe}_3\text{O}_4$ , (b) PGMA- $\text{Fe}_3\text{O}_4$ , (c) DAAO-PGMA- $\text{Fe}_3\text{O}_4$ , and (d) high-resolution TEM image of DAAO-PGMA- $\text{Fe}_3\text{O}_4$ .

$11.6 \pm 2.2$  nm. After modification of PGMA and DAAO, the size of nanoparticles did not obviously change in TEM images. It was speculated that the PGMA shell could not be easily distinguished in TEM images due to the low contrast between PGMA and the background,<sup>27,51</sup> but its presence was still evidenced by the obtained results of FT-IR spectroscopy. Moreover, the magnetite nanoparticles are dispersed better than unfunctional ones after modification with PGMA and DAAO, and a thin layer also could be observed, indicating the successful functionality of the  $\text{Fe}_3\text{O}_4$  nanoparticles.

The magnetic properties of the prepared nanoparticles were investigated via a VSM. Figure 4 displays the magnetization of

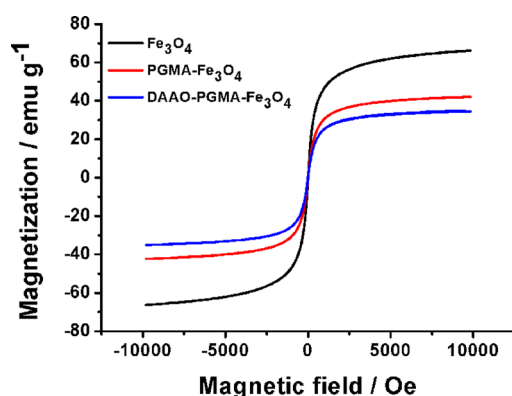


**Figure 4.** Magnetization curves of magnetic  $\text{Fe}_3\text{O}_4$ , PGMA- $\text{Fe}_3\text{O}_4$ , and DAAO-PGMA- $\text{Fe}_3\text{O}_4$  nanoparticles at 25 °C.

the as-prepared magnetic nanoparticles at room temperature. The saturation magnetization of the magnetic  $\text{Fe}_3\text{O}_4$ , PGMA- $\text{Fe}_3\text{O}_4$ , and DAAO-PGMA- $\text{Fe}_3\text{O}_4$  are 66.228, 23.453, and 19.434 emu/g, respectively. The results reveal that the magnetism of the nanoparticles decreases with stepwise modification and that longer time is required for complete magnetic capture (Figure S2, Supporting Information).<sup>27,52</sup> However, these synthesized nanoparticles also could be well separated from the bulk solution phase within 30 s when an external magnet is introduced at the bottom of the vial (Figure

S2, Supporting Information). In addition, these magnetic nanoparticles have very low coercivity and no obvious hysteresis, which demonstrates a typical characteristic of superparamagnetic behavior at room temperature.<sup>53,54</sup> The results demonstrate that the prepared nanoparticles possess remarkable magnetic responsiveness, which is an advantage in the separation and reusability of the immobilized enzyme in practical applications.

**3.2. Application.** After successful construction of the DAAO reactor, an efficient CLE-CE system with AAIL as chiral ligand was developed for monitoring the enzymatic activity of the enzyme reactor and was further applied in exploring the DAAO inhibitors. In this work, new AAIL [ $\text{P}_{1.4}$ ][L-Orn] was synthesized (Scheme S1, Supporting Information), and its structure was characterized by NMR (Supporting Information, section 2). Then, it was subsequently employed as a new chiral ligand in the proposed CLE-CE system, and several key chiral separation parameters, including buffer pH, concentration ratio of central ion to ligand, and concentration of chiral selector, were optimized with Dns-D,L-Ile, Dns-D,L-Met, Dns-D,L-Ser as the test analytes. All the optimization results are displayed in Supporting Information (Figures S3–S6). Finally, under the optimum conditions, Dns-D,L-Ile, Dns-D,L-Met, Dns-D,L-Ser, and several other pairs of the labeled AA enantiomers were effectively separated (Figures S7 and S8, and Table S1, Supporting Information). The results demonstrated that the proposed CLE-CE system could be effectively employed in DAAO kinetics studies and inhibitor screening using D,L-Met as the efficient substrate of DAAO.<sup>18</sup> Moreover, this method was validated with favorable quantitation features (Supporting Information, section 5.2 and Figure S9); thus, it was further applied in the monitoring of the DAAO-mediated catalytic reaction and screening of DAAO inhibitors in this study.

**3.2.1. Enzymolysis.** To utilize the as-prepared PGMA-functionalized magnetic nanoparticles for enzymolysis and enzyme inhibitor screening, DAAO was immobilized onto the magnetic PGMA- $\text{Fe}_3\text{O}_4$  nanoparticles. The immobilized amount of DAAO on the PGMA- $\text{Fe}_3\text{O}_4$  nanoparticles was determined by the classical coomassie blue-binding assay. For accurate calculation of the immobilized amount, a calibration curve was obtained by determining the absorbance of the standard DAAO solutions in a range of 0.078–5.0 mg/mL at 595 nm by incubating with Coomassie brilliant blue G-250 solution, and the obtained calibration curve is displayed in Figure S10 (Supporting Information). After monitoring the absorbance at 595 nm of the supernatant before and after immobilization, the immobilized amounts of DAAO were calculated according to the calibration curve, and the data are summarized in Table 1. The results demonstrated that the immobilized amounts of DAAO were enhanced (from 94.0 to 222.0  $\mu\text{g}/\text{mg}$  nanoparticle) with increasing lengths of polymer brushes due to the increase in reaction sites provided by the reactive polymer brushes. Finally,  $\text{Fe}_3\text{O}_4$ -PGMA<sub>193</sub> was chosen for further application since the immobilization efficiency reached 88.6%. Compared with other reported systems in the literature,<sup>18,55,56</sup> our synthesized polymer modified magnetic nanoparticles are favorable for increased immobilization amounts of enzyme. The results indicated that the polymer modified magnetic nanoparticles are favorable for the effective immobilization of enzyme in high loading capacity (222.0  $\mu\text{g}/\text{mg}$  nanoparticle).

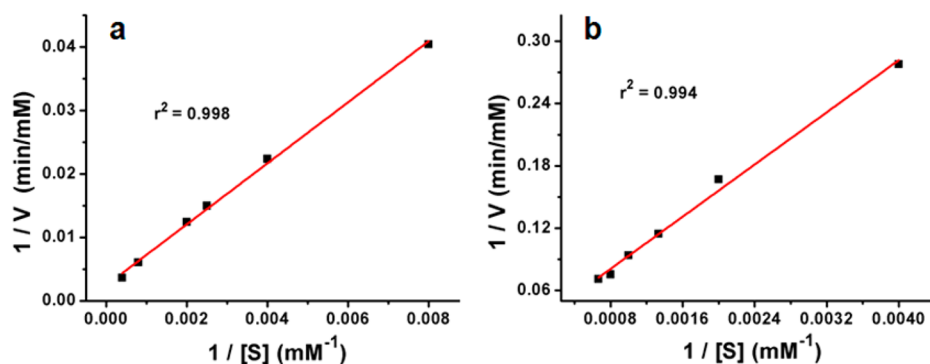


Figure 5. Lineweaver–Burk plot for (a) DAAO immobilized magnetic nanoparticles modified with a reactive polymer and (b) free enzyme solution.

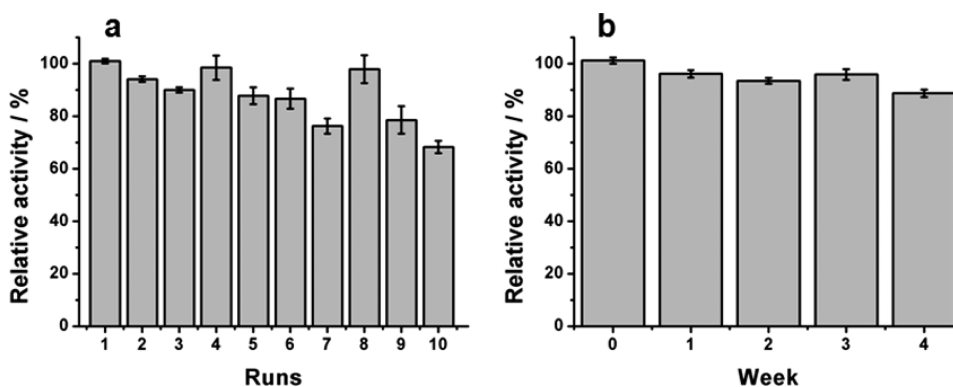


Figure 6. Reusability (a) and stability (b) test of DAAO immobilized magnetic nanoparticles modified with a reactive polymer.

D-Met has been testified to be the efficient substrate of DAAO enzyme for evaluation of the performance of the immobilized DAAO.<sup>31,32</sup> Thus, the values of the Michaelis constant ( $K_m$ , which reflects the enzymatic affinities) and the maximum velocity ( $V_{max}$ , which represents the activity of the enzyme reactors) are investigated to examine the enzymatic bioactivity of the immobilized DAAO reactors using D-Met as the substrate. The values could be calculated by plotting the initial reaction rate to the injected substrate concentrations and deriving from a linearized form of the Michaelis–Menten equation:<sup>57–59</sup>

$$[S]/\nu = K_m/V_{max} + [S]/V_{max} \quad (4)$$

where  $\nu$  is the velocity of the enzymatic activity, and  $[S]$  is the concentration of the substrate.

Figure 5a shows the plots for the conversion of D-Met in the enzymatic reactors, and the corresponding  $K_m$  and  $V_{max}$  were calculated to be 2.4 mM and 500  $\mu\text{M min}^{-1}$  ( $\text{mg of DAAO}^{-1}$ ), respectively. For comparison, the kinetic characteristics of free enzyme in solution were also investigated, and the values were calculated to be 2.1 mM for  $K_m$  and 33.3  $\mu\text{M min}^{-1}$  ( $\text{mg of DAAO}^{-1}$ ) for  $V_{max}$ , separately (Figure 5b). It has been found that the  $K_m$  value of the immobilized reactor (2.4 mM) is a little higher than that of free DAAO (2.1 mM), which could be ascribed to the decrease in mass transfer within the polymer shell, and this phenomenon was often observed within the immobilized enzyme systems.<sup>27,57–59</sup> However, the  $V_{max}$  value of the immobilized DAAO is about 15 times higher than that of the free DAAO, which means that a higher reaction rate for the immobilized reactor can be obtained at a similar concentration of D-Met.<sup>44</sup> This result can be explained as follows: the large amount of DAAO concentrated in a very limited space, and the

decreased diffusion within the matrix also increases the frequency of interaction between DAAO and substrates.<sup>60,61</sup>

The reusability of the immobilized enzyme was studied by incubating the substrate D-Met with the same group of the magnetic DAAO-PGMA- $\text{Fe}_3\text{O}_4$  nanoparticles repeatedly, and the results are displayed in Figure 6a. The immobilized DAAO retained above 68.2% residual activity after 10 consecutive operations. The result revealed that the DAAO immobilized on polymer-functionalized  $\text{Fe}_3\text{O}_4$  nanoparticles showed good reusability. Moreover, DAAO immobilized on magnetic nanoparticles maintained significant activity (more than 88.7%) after 4-weeks of storage at 4 °C (50.0 mM Tris-HCl, pH 8.2), as shown in Figure 6b. However, under the same storage conditions, the fall in activity of the free enzyme amounted to 89.4% within 24 h. The results showed that the immobilized DAAO had better storage stability than the free enzyme. It has been reported that the immobilization of an enzyme to a carrier often limits its freedom to undergo drastic conformational changes; thus, it would result in increased stability toward denaturation.<sup>62</sup>

**3.2.2. Immobilized DAAO Magnetic Nanoparticles for Screening Enzyme Inhibitors.** One of the most potential applications of the enzyme immobilized magnetic nanoparticles is in determining and identifying enzyme inhibitors.<sup>4</sup> It is widely accepted that benzoic acid and its derivatives are marked and selective inhibitors of DAAO. In this study, benzoic acid and various monosubstituted benzoic acid derivatives were used to evaluate the function of the immobilized DAAO magnetic nanoparticles. It could be found that the enzyme activity was obviously inhibited after the introduction of benzoic acid (Figure S11, Supporting Information) and that the enzyme activity decreased with the increasing of the concentration of

inhibitors. The  $IC_{50}$  for the 10 inhibitors was determined at a substrate concentration of  $333.3 \mu\text{M}$ , and the results are listed in Table 2. By comparing the  $IC_{50}$  values of the inhibitors, the

**Table 2. Results of  $IC_{50}$  and  $K_I$  for 10 DAAO inhibitors**

inhibitors	$IC_{50}$ (M)	$K_I$ (M)
benzoic acid	$1.3 \times 10^{-4}$	$3.5 \times 10^{-5}$
benzamide	$1.1 \times 10^{-2}$	$5.9 \times 10^{-3}$
2-hydroxybenzoic acid	$6.5 \times 10^{-4}$	$2.2 \times 10^{-4}$
3-hydroxybenzoic acid	$8.0 \times 10^{-4}$	$6.6 \times 10^{-4}$
4-hydroxybenzoic acid	$4.6 \times 10^{-3}$	$2.1 \times 10^{-3}$
2-nitrobenzoic acid	$1.7 \times 10^{-2}$	$7.8 \times 10^{-3}$
3-nitrobenzoic acid	$7.2 \times 10^{-4}$	$6.3 \times 10^{-4}$
4-nitrobenzoic acid	$6.8 \times 10^{-4}$	$4.6 \times 10^{-4}$
2-aminobenzoic acid	$9.7 \times 10^{-4}$	$7.1 \times 10^{-4}$
4-aminobenzoic acid	$8.9 \times 10^{-3}$	$3.4 \times 10^{-3}$

order of their inhibitory potency is as follows: benzoic acid > 2-hydroxybenzoic acid > 4-nitrobenzoic acid > 3-nitrobenzoic acid > 3-hydroxybenzoic acid > 2-aminobenzoic acid > 4-hydroxybenzoic acid > 4-aminobenzoic acid > benzamide > 2-nitrobenzoic acid. Moreover, the  $K_I$  of each inhibitor was determined by extrapolation of  $IC_{50}$  values (at four different concentrations of substrate) to the point of the substrate concentration of zero according to eq 2, and the results are presented in Table 1. It should be noted that each of the samples was assayed in triplicate, and the relative standard deviation (RSD,  $n = 3$ ) was in the range from 0.1 to 5.7%. Meanwhile, the calculated values of  $IC_{50}$  and  $K_I$  were in agreement with the general outcomes of the literature.<sup>7,63</sup> Importantly, both the  $IC_{50}$  and  $K_I$  results indicated that benzoic acid had a markedly stronger inhibitive effect among the 10 inhibitors, which was consistent with the previous literature<sup>63</sup> and demonstrated that the prepared magnetic DAAO-PGMA- $Fe_3O_4$  reactor exhibited good potential in evaluating the inhibition efficiency of DAAO inhibitors.

The reusability of the immobilized enzyme for screening the inhibitors of DAAO was assessed by carrying out 10 sequential enzymatic incubations using the same immobilized enzyme with benzoic acid as the model inhibitor. As shown in Figure 7, the results displayed that the obtained inhibition efficiency of benzoic acid was not obviously changed after 10 runs and that the relative standard deviation (RSD) was calculated to be

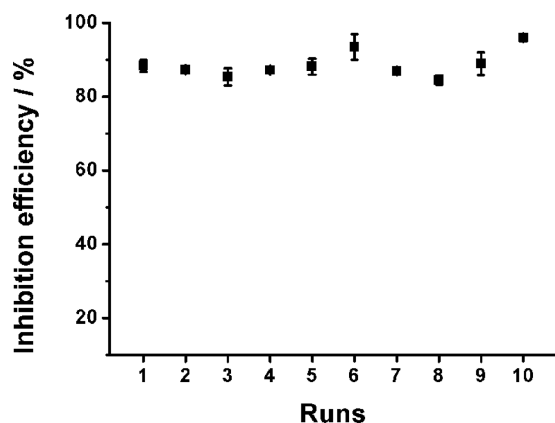


**Figure 7.** Reusability test of the immobilized magnetic nanoparticles modified with a reactive polymer for screening the inhibitors of DAAO.

4.3%, indicating the satisfactory applicability of the prepared DAAO-modified magnetic nanoparticle in studying enzyme inhibitors.

## 4. CONCLUSIONS

In this work, DAAO was successfully immobilized onto the surface of the magnetic nanoparticles, which was modified by the biocompatible reactive polymer PGMA. To overcome the limitation of the conventional synthesis process which needed quite a long reaction time between enzyme and PGMA,  $LiClO_4$  was employed as the effective catalyst for the activation of epoxides, and it could obviously shorten the immobilization time of DAAO. Meanwhile, a new CLE-CE system with AAIL  $[P_{1,4}][Orn]$  as chiral ligand was constructed for separation of the substrate AAs and further employed in evaluating the immobilized DAAO magnetic nanoparticles. The immobilized biocatalyst has been successfully applied in screening the enzyme inhibitors and presented high enzymatic activity, good reusability, and satisfactory stability. This proposed protocol provides a facile and efficient approach to fabricate the enzyme-functionalized magnetic nanoparticles modified by a reactive polymer for screening the inhibitors of DAAO. Moreover, it can be subsequently adapted to immobilization of other enzymes and potentially realizing the high-throughput screening of enzyme inhibitors.

## ■ ASSOCIATED CONTENT

### Supporting Information

Synthesis procedure of  $[P_{1,4}][Orn]$ , NMR characterization of  $[P_{1,4}][Orn]$ , SDS-PAGE analysis of DAAO, photographs of an aqueous suspension of magnetic nanoparticles, separation conditions and sample preparation, derivatization process, quantitation feature of the CLE-CE system, separation condition optimization, electropherogram of Dns-D,L-Ile, Dns-D,L-Met, Dns-D,L-Ser, Dns-D,L-Cys, Dns-D,L-Tyr, Dns-D,L-Phe, and Dns-D,L-Thr under optimum conditions, electropherogram of the limits of detection (LODs) for Dns-D-Met and Dns-L-Met, enantioseparation results of Dns-D,L-AAAs under the optimum conditions, the calibration curve of DAAO by the classical Coomassie blue-binding assay, and electropherograms of Dns-DL-Met after incubation with the immobilized DAAO reactor at  $37 \text{ }^\circ\text{C}$  for 5 min in the presence or absence of benzoic acid. This material is available free of charge via the Internet at <http://pubs.acs.org>.

## ■ AUTHOR INFORMATION

### Corresponding Author

\*Tel: +86-10-82627290. Fax: +86-10-62559373. E-mail: qili@iccas.ac.cn.

### Notes

The authors declare no competing financial interest.

## ■ ACKNOWLEDGMENTS

We acknowledge financial support from the NSFC (No. 21375132, No. 21175138, No. 21135006, No. 21205125, and No. 21321003). Also, we greatly appreciate Dr. Ping Dong and Professor Ran Xiao for their kind help with the SDS-PAGE analysis.

## REFERENCES

- (1) Pollegioni, L.; Piubelli, L.; Sacchi, S.; Pilone, M. S.; Molla, G. Physiological Functions of D-Amino Acid Oxidases: from Yeast to Humans. *Mol. Life Sci.* **2007**, *64*, 1373–1394.
- (2) Vanoni, M. A.; Cosma, A.; Mazzeo, D.; Mattevi, A.; Todone, F.; Curti, B. Limited Proteolysis and X-Ray Crystallography Reveal the Origin of Substrate Specificity and of the Rate-Limiting Product Release during Oxidation of D-Amino Acids Catalyzed by Mammalian D-Amino Acid Oxidase. *Biochemistry* **1997**, *36*, 5624–5632.
- (3) Khoronenkova, S. V.; Tishkov, V. I. D-Amino Acid Oxidase: Physiological Role and Applications. *Biochemistry (Moscow)* **2008**, *73*, 1511–1518.
- (4) Ferraris, D. V.; Tsukamoto, T. Recent Advances in the Discovery of D-Amino Acid Oxidase Inhibitors and Their Therapeutic Utility in Schizophrenia. *Curr. Pharm. Des.* **2011**, *17*, 103–111.
- (5) Fukumoto, K.; Yoshizawa, M.; Ohno, H. Room Temperature Ionic Liquids from 20 Natural Amino Acids. *J. Am. Chem. Soc.* **2005**, *127*, 2398–2399.
- (6) Liu, Q.; Wu, K. K.; Tang, F.; Yao, L. H.; Yang, F.; Nie, Z.; Yao, S. Z. Amino Acid Ionic Liquids as Chiral Ligands in Ligand-Exchange Chiral Separations. *Chem.—Eur. J.* **2009**, *15*, 9889–9896.
- (7) Bartlett, G. R. The Inhibition of D-Amino Acid Oxidase by Benzoic Acid and Various Monosubstituted Benzoic Acid Derivatives. *J. Am. Chem. Soc.* **1948**, *70*, 1010–1011.
- (8) Ferraris, D.; Duvall, B.; Ko, Y. S.; Thomas, A. G.; Rojas, C.; Majer, P.; Hashimoto, K.; Tsukamoto, T. Synthesis and Biological Evaluation of D-Amino Acid Oxidase Inhibitors. *J. Med. Chem.* **2008**, *51*, 3357–3359.
- (9) Adage, T.; Trillat, A. C.; Quattropani, A.; Perrin, D.; Cavarec, L.; Shaw, J.; Guerassimenko, O.; Giachetti, C.; Gréco, B.; Chumakov, I.; Halazy, S.; Roach, A.; Zaratin, P. In Vitro and in Vivo Pharmacological Profile of AS057278, A Sselective D-Amino Acid Oxidase Inhibitor with Potential Anti-Psychotic Properties. *Eur. Neuropsychopharm.* **2008**, *18*, 200–214.
- (10) Oguri, S.; Watanabe, K.; Nozu, A.; Kamiya, A. Screening of D-Amino Acid Oxidase Inhibitor by A New Multi-Assay Method. *Food Chem.* **2007**, *100*, 616–622.
- (11) Gong, N.; Gao, Z. Y.; Wang, Y. C.; Li, X. Y.; Huang, J. L.; Hashimoto, K.; Wang, Y. X. A Series of D-Amino Acid Oxidase Inhibitors Specifically Prevents and Reverses Formalin-Induced Tonic Pain in Rats. *J. Pharmacol. Exp. Ther.* **2011**, *336*, 282–293.
- (12) Caldinelli, L.; Molla, G.; Bracci, L.; Lelli, B.; Pileri, S.; Cappelletti, P.; Sacchi, S.; Pollegioni, L. Effect of Ligand Binding on Human D-Amino Acid Oxidase: Implications for the Development of New Drugs for Schizophrenia Treatment. *Protein Sci.* **2010**, *19*, 1500–1512.
- (13) Hodgson, R. J.; Besanger, T. R.; Brook, M. A.; Brennan, J. D. Inhibitor Screening Using Immobilized Enzyme Reactor Chromatography/Mass Spectrometry. *Anal. Chem.* **2005**, *77*, 7512–7519.
- (14) Cao, M.; Li, Z. H.; Wang, J. L.; Ge, W. P.; Yue, T. L.; Li, R. H.; Colvin, V. L.; Yu, W. W. Food Related Applications of Magnetic Iron Oxide Nanoparticles: Enzyme Immobilization, Protein Purification, and Food Analysis. *Trends Food Sci. Technol.* **2012**, *27*, 47–56.
- (15) Brady, D.; Jordaan, J. Advances in Enzyme Immobilisation. *Biotechnol. Lett.* **2009**, *31*, 1639–1650.
- (16) Sheldon, R. A.; Pelt, S. V. Enzyme Immobilisation in Biocatalysis: Why, What and How. *Chem. Soc. Rev.* **2013**, *42*, 6223–6235.
- (17) López-Gallego, F.; Betancor, L.; Hidalgo, A.; Alonso, N.; Fernandez-Lorente, G.; Guisan, J. M.; Fernandez-Lafuente, R. Preparation of a Robust Biocatalyst of D-Amino Acid Oxidase on Sepabeads Supports Using the Glutaraldehyde Crosslinking Method. *Enzyme Microb. Technol.* **2005**, *37*, 750–756.
- (18) Bava, A.; Gornati, R.; Cappellini, F.; Caldinelli, L.; Pollegioni, L.; Bernardini, G. D-Amino Acid Oxidase-Nanoparticle System: A Potential Novel Approach for Cancer Enzymatic Therapy. *Nanomedicine* **2013**, *8*, 1797–1806.
- (19) Vasyliava, N.; Barnych, B.; Meillerd, A.; Mauclera, C.; Pollegioni, L.; Lina, J. S.; Barbier, D.; Marinesco, S. Covalent Enzyme Immobilization by Poly(ethylene glycol) Diglycidyl ether (PEGDE) for Microelectrode Biosensor Preparation. *Biosens. Bioelectron.* **2011**, *26*, 3993–4000.
- (20) Hsieh, H. C.; Kuan, I. C.; Lee, S. L.; Tien, G. Y.; Wang, Y. J.; Yu, C. Y. Stabilization of D-Amino Acid Oxidase from *Rhodospiridium Toruloides* by Immobilization onto Magnetic Nanoparticles. *Biotechnol. Lett.* **2009**, *31*, 557–563.
- (21) Kim, J.; Grate, J. W.; Wang, P. Nanostructures for Enzyme Stabilization. *Chem. Eng. Sci.* **2006**, *61*, 1017–1026.
- (22) Qin, W. J.; Song, Z. F.; Fan, C.; Zhang, W. J.; Cai, Y.; Zhang, Y. J.; Qian, X. H. Trypsin Immobilization on Hairy Polymer Chains Hybrid Magnetic Nanoparticles for Ultra Fast, Highly Efficient Proteome Digestion, Facile <sup>18</sup>O Labeling and Absolute Protein Quantification. *Anal. Chem.* **2012**, *84*, 3138–3144.
- (23) Tsang, S. C.; Yu, C. H.; Gao, X.; Tam, K. Silica-Encapsulated Nanomagnetic Particle as A New Recoverable Biocatalyst Carrier. *J. Phys. Chem. B* **2006**, *110*, 16914–16922.
- (24) Prakasham, R. S.; Devi, G. S.; Laxmi, K. R.; Rao, C. S. Novel Synthesis of Ferric Impregnated Silica Nanoparticles and Their Evaluation as A Matrix for Enzyme Immobilization. *J. Phys. Chem. C* **2007**, *111*, 3842–3847.
- (25) Huang, J. S.; Han, B. Z.; Yue, W.; Yan, H. S. Magnetic Polymer Microspheres with Polymer Brushes and the Immobilization of Protein on the Brushes. *J. Mater. Chem.* **2007**, *17*, 3812–3818.
- (26) Huang, J. S.; Li, X. T.; Zheng, Y. H.; Zhang, Y.; Zhao, R. Y.; Gao, X. G.; Yan, H. S. Immobilization of Penicillin G Acylase on Poly[(glycidyl methacrylate)-co-(glycerol monomethacrylate)]-Grafted Magnetic Microspheres. *Macromol. Biosci.* **2008**, *8*, 508–515.
- (27) Shen, Y.; Guo, W.; Qi, L.; Qiao, J.; Wang, F. Y.; Mao, L. Q. Immobilization of Trypsin via Reactive Polymer Grafting from Magnetic Nanoparticles for Microwave-Assisted Digestion. *J. Mater. Chem. B* **2013**, *1*, 2260–2267.
- (28) Azizi, N.; Mirmashhori, B.; Saidi, M. R. Lithium Perchlorate Promoted Highly Regioselective Ring Opening of Epoxides under Solvent-Free Conditions. *Catal. Commun.* **2007**, *8*, 2198–2203.
- (29) Azizi, N.; Saidi, M. R. Solid Lithium Perchlorate as A Powerful Catalyst for the Synthesis of  $\beta$ -Aminoalcohols under Solvent-Free Conditions. *Can. J. Chem.* **2005**, *83*, 505–507.
- (30) Abae, M. S.; Mojtahedi, M. M.; Abbasi, H.; Fatemi, E. R. Additive-Free Thiolytic Pathway of Epoxides in Water: A Green and Efficient Regioselective Pathway to  $\beta$ -Hydroxy Sulfides. *Synth. Commun.* **2008**, *38*, 282–289.
- (31) Zhang, H. Z.; Qi, L.; Lin, Y. Q.; Mao, L. Q.; Chen, Y. Study on the Decrease of Renal D-Amino Acid Oxidase Activity in the Rat After Renal Ischemia by Chiral Ligand Exchange Capillary Electrophoresis. *Amino Acids* **2012**, *42*, 337–345.
- (32) Mu, X. Y.; Qi, L.; Shen, Y.; Zhang, H. Z.; Qiao, J.; Ma, H. M. A Novel Chiral Ligand Exchange Capillary Electrophoresis System with Amino Acid Ionic Liquid as Ligand and Its Application in Screening D-Amino Acid Oxidase Inhibitors. *Analyst* **2012**, *137*, 4235–4240.
- (33) Massart, R.; Cabuil, V. Effect of Some Parameters on the Formation of Colloidal Magnetite in Alkaline Medium: Yield and Particle Size Control. *J. Chim. Phys. Phys.-Chim. Biol.* **1987**, *84*, 967–973.
- (34) Asryants, R. A.; Duszenkova, I. V.; Nagradova, N. K. Determination of Sepharose-Bound Protein with Coomassie Brilliant Blue G-250. *Anal. Biochem.* **1985**, *151*, 571–574.
- (35) Bradford, M. M. A Rapid and Sensitive Method for the Quantitation of Microgram Quantities of Protein Utilizing the Principle of Protein-Dye Binding. *Anal. Biochem.* **1976**, *72*, 248–254.
- (36) Cui, Y. J.; Chen, X.; Li, Y. F.; Liu, X.; Lei, L.; Xuan, S. T. Novel Magnetic Microspheres of P(GMA-b-HEMA): Preparation, Lipase Immobilization and Enzymatic Activity in Two Phases. *Appl. Microbiol. Biotechnol.* **2012**, *95*, 147–156.
- (37) Chou, T. C.; Hsu, W.; Wang, C. H.; Chen, Y. J.; Fang, J. M. Rapid and Specific Influenza Virus Detection by Functionalized Magnetic Nanoparticles and Mass Spectrometry. *J. Nanobiotechnol.* **2011**, *9*, 52.



- (38) Zhang, H. Z.; Qi, L.; Qiao, J.; Mao, L. Q. Determination of Sodium Benzoate by Chiral Ligand Exchange CE Based on Its Inhibitory Activity in D-Amino Acid Oxidase Mediated Oxidation of D-Serine. *Anal. Chim. Acta* **2011**, *691*, 103–109.
- (39) Wang, M.; Gu, X. G.; Zhang, G. X.; Zhang, D. Q.; Zhu, D. B. Convenient and Continuous Fluorometric Assay Method for Acetylcholinesterase and Inhibitor Screening Based on the Aggregation-Induced Emission. *Anal. Chem.* **2009**, *81*, 4444–4449.
- (40) Cheng, Y. C.; Prusoff, W. H. Relationship between the Inhibition Constant ( $K_i$ ) and the Concentration of Inhibitor Which Causes 50% Inhibition ( $I_{50}$ ) of an Enzymatic Reaction. *Biochem. Pharmacol.* **1973**, *22*, 3099–3108.
- (41) Lizcano, J. M.; Arriba, A. F. D.; Tipton, K. F.; Unzeta, M. Inhibition of Bovine Lung Semicarbazide Sensitive Amine Oxidase (SSAO) by Some Hydrazine Derivatives. *Biochem. Pharmacol.* **1996**, *52*, 187–195.
- (42) Zhou, L. L.; Yuan, J. Y.; Yuan, W. Z.; Sui, X. F.; Wu, S. Z.; Li, Z. L.; Shen, D. Z. Synthesis, Characterization, and Controllable Drug Release of pH-Sensitive Hybrid Magnetic Nanoparticles. *J. Magn. Mater.* **2009**, *321*, 2799–2804.
- (43) Ganesan, A. Integrating Natural Product Synthesis and Combinatorial Chemistry. *Pure Appl. Chem.* **2001**, *73*, 1033–1039.
- (44) Montigny, P. D.; Stobaugh, J. F.; Givens, R. S.; Carlson, R. G.; Srinivasachar, K.; Sternson, L. A.; Higuchi, T. Naphthalene-2,3-dicarboxyaldehyde/cyanide Ion: A Rationally Designed Fluorogenic Reagent for Primary Amines. *Anal. Chem.* **1987**, *59*, 1096–1101.
- (45) Tu, S. C.; Edelstein, S. J.; McCormick, D. B. A Modified Purification Method and Properties of Pure Porcine D-Amino Acid Oxidase. *Arch. Biochem. Biophys.* **1973**, *159*, 889–896.
- (46) Curti, B.; Ronchi, S.; Branzoli, U.; Ferri, G.; Williams, C. H. Improved Purification, Amino Acid Analysis and Molecular Weight of Homogeneous D-Amino Acid Oxidase from Pig Kidney. *Biochim. Biophys. Acta* **1973**, *327*, 266–273.
- (47) Schröder, T.; Andreesen, J. R. Evidence for the Functional Importance of Cys298 in D-Amino Acid Oxidase from *Trigonopsis Variabilis*. *Eur. J. Biochem.* **1993**, *218*, 735–744.
- (48) Pollegioni, L.; Simonetta, M. P. Immunochemical Studies on *Rhodotrovula gracilis* D-Amino Acid Oxidase. *Experientia* **1991**, *47*, 232–235.
- (49) Gelbrich, T.; Feyen, M.; Schmidt, A. M. Magnetic Thermoresponsive Core Shell Nanoparticles. *Macromolecule* **2006**, *39*, 3469–3472.
- (50) Ma, Z. Y.; Guan, Y. P.; Liu, H. Z. Synthesis of Monodisperse Nonporous Crosslinked Poly(glycidyl methacrylate) Particles with Metal Affinity Ligands for Protein Adsorption. *Polym. Int.* **2005**, *54*, 1502–1507.
- (51) Luo, B.; Song, X. J.; Zhang, F.; Xia, A.; Yang, W. L.; Hu, J. H.; Wang, C. C. Multi-Functional Thermosensitive Composite Microspheres with High Magnetic Susceptibility Based on Magnetite Colloidal Nanoparticle Clusters. *Langmuir* **2010**, *26*, 1674–1679.
- (52) Wang, S. M.; Su, P.; Huang, J.; Wu, J. W.; Yang, Y. Magnetic Nanoparticles Coated with Immobilized Alkaline Phosphatase for Enzymolysis and Enzyme Inhibition Assays. *J. Mater. Chem. B* **2013**, *1*, 1749–1754.
- (53) Ren, Q.; Chu, H.; Chen, M. Q.; Ni, Z. B.; Chen, Q. Y. Design and Fabrication of Superparamagnetic Hybrid Microspheres for Protein Immobilization. *J. Wuhan Univ. Technol.* **2011**, *26*, 1084–1088.
- (54) Wan, S. R.; Zheng, Y.; Liu, Y. Q.; Yan, H. S.; Liu, K. L.  $Fe_3O_4$  Nanoparticles Coated with Homopolymers of Glycerol Mono(meth)acrylate and Their Block Copolymers. *J. Mater. Chem.* **2005**, *15*, 3424–3430.
- (55) Lin, S.; Yun, D.; Qi, D. W.; Deng, C. H.; Li, Y.; Zhang, X. M. Novel Microwave-Assisted Digestion by Trypsin-Immobilized Magnetic Nanoparticles for Proteomic Analysis. *J. Proteome Res.* **2008**, *7*, 1297–1307.
- (56) Krogh, T. N.; Berg, T.; Højrup, P. Protein Analysis Using Enzymes Immobilized to Paramagnetic Beads. *Anal. Biochem.* **1999**, *274*, 153–162.
- (57) Wu, H. L.; Tian, Y. P.; Liu, B. H.; Lu, H. J.; Wang, X. Y.; Zhai, J. J.; Jin, H.; Yang, P. Y.; Xu, Y. M.; Wang, H. H. Titania and Alumina Sol–Gel-Derived Microfluidics Enzymatic-Reactors for Peptide Mapping: Design, Characterization, and Performance. *J. Proteome Res.* **2004**, *3*, 1201–1209.
- (58) Huang, Y.; Shan, W.; Liu, B. H.; Liu, Y.; Zhang, Y. H.; Zhao, Y.; Lu, H. J.; Tang, Y.; Yang, P. Y. Zeolite Nanoparticle Modified Microchip Reactor for Efficient Protein Digestion. *Lab Chip* **2006**, *6*, 534–539.
- (59) Xie, S. F.; Svec, F.; Fréchet, J. M. J. Design of Reactive Porous Polymer Supports for High Throughput Bioreactors: Poly(2-vinyl-4,4-dimethylazlactone-co-acrylamide-co-ethylene dimethacrylate) Monoliths. *Biotechnol. Bioeng.* **1999**, *62*, 30–35.
- (60) Bi, H. Y.; Qiao, L.; Busnel, J. M.; Liu, B. H.; Girault, H. H. Kinetics of Proteolytic Reactions in Nanoporous Materials. *J. Proteome Res.* **2009**, *8*, 4685–4692.
- (61) Jiang, D. S.; Long, S. Y.; Huang, J.; Xiao, H. Y.; Zhou, J. Y. Immobilization of *Pycnoporus Sanguineus* Laccase on Magnetic Chitosan Microspheres. *Biochem. Eng. J.* **2005**, *25*, 15–23.
- (62) Leonowicz, A.; Sarkar, J. M.; Bollag, J. M. Improvement in Stability of an Immobilized Fungal Laccase. *Appl. Microbiol. Biotechnol.* **1988**, *29*, 129–135.
- (63) Vanoni, M. A.; Cosma, A.; Mazzeo, D.; Mattevi, A.; Todone, F.; Curti, B. Limited Proteolysis and X-ray Crystallography Reveal the Origin of Substrate Specificity and of the Rate-Limiting Product Release during Oxidation of D-Amino Acids Catalyzed by Mammalian D-Amino Acid Oxidase. *Biochemistry* **1997**, *36*, 5624–5632.